

ENERGY SAVING AND VOLTAGE STABILISATION IN URBAN ELECTRIFIED PUBLIC TRANSPORT OF BELGRADE – ANALYSIS OF SIMULATION RESULTS

Gavrilovic Branislav¹, PhD; Bundalo Zoran², PhD

¹ Railway College of Vocational Studies, Belgrade, SERBIA, gavrilovicbranislav5@gmail.com

² Railway College of Vocational Studies, Belgrade, SERBIA, cheminot2@gmail.com

Abstract: The power consumption of a tram is characterized by distinct peaks combined with a low average value. Using an on-board energy storage, the overhead line peak power and energy consumption can be reduced. The storage device introduces a degree of freedom for control of the power flow. To incorporate the freedom an energy management is required. The design of the energy management can be seen as a multi-objective optimization problem with the objectives “minimize line peak power” and “minimize energy consumption”. As common to most multiobjective optimization problems it is not possible to minimize both objectives at the same time.

This paper describes new on board energy storage systems applied in the urban electrified public transport in Belgrade (R. Serbia)

Keywords: regenerative brak , energy consumption savings

1. INTRODUCTION

The urban electrified public transport in Belgrade, employ the low voltage DC systems at 600 V, which are usually the most economic. In this case, the pantograph connects directly the contact line to the power inverters of the train by means of filter capacitors. The average distance between substations is very limited for example, in a subway at 750 V with heavy traffic, it can be of the order of 1.5 km, with minimum values of 1.3 km.

The urban electrified public transport in Belgrade, employ the low voltage DC systems at 600 V. Tram system is a 1000 mm gauge network that in 2016 had 10 routes running on 43.5 kilometres of (at least mostly double) track in the city of Belgrade, the capital of Serbia. It is operated with around 200 trams, including 30 the electrical multiple unit train manufactured by CAF S.A. (Construcciones y Auxiliar de Ferrocarriles) named CAF Urbos 3 (see figure 1).



Figure 1: Picture of CAF Urbos 3 electrical multiple units operating on of Belgrade Urban Line

The main parametars of the CAF Urbos 3 are: Architecture- Mc-S-R-S-Mc, Rated power- 560 kW, Tram length: 31380 mm, Tram width- 2400 mm, Tram height- 3350 mm, Number of passengers: 261, Max. speed- 70 km/h, Acceleration - (0-35 km/h): 1.2 m/s², Traction power - 750V, Emergency brake deceleration rate – 2,8 m/s².

Urban transit network of Belgrade with the CAF Urbos 3 applied mobile energy storage system (or so called on-board energy storage systems), which consists of onboard energy storage systems usually located on the tram roof. Every system works independently, and the recovered energy is directly sent to the storage system placed on the tram. CAF Urbos 3 has been developing its ACR (Rapid Charge Accumulator) overhead contact system in conjunction with Tranelec and Aragon Technical Institute [1].

The super-capacitors can be fully charged, while the train is stopped in a station, in around 20 seconds [1]. In addition, as for the rest of technologies, the system recovers the energy stored on the journey and the braking energy too [2].

The roof-mounted accumulator is suitable for rolling stock of any manufacturer, as well as any new or existing installations or infrastructure [2]. It can be complemented with NiMH batteries as backup for solving super-capacitor’s failure situations.

The implementation of ACR in a light rail vehicle increases its weight around 2 t per module.

With the common solution for overhead contact -free systems of two modules, this leads to an increase of 4 t. The increase of weight is compensated with the energy saving.

The system has been tested during one year, in a first stage in Vélez-Málaga, and in May 2010, the first tram provided with ACR initiated its commercial service in Seville (Spain). These vehicles will allow the overhead contact system to be definitely eliminated in the whole Seville network but at stations [3].

CAF Urbos 3 assures that these vehicles can achieve a maximum autonomy of 1000 m, but in the commercial service 500 m are guaranteed with active auxiliary systems [3].

In relation to vehicle’s overcost due to super-capacitor provision, CAF assures that in the next developments it can be around 10-15%. Super-capacitor’s life depends on temperatures and charge/uncharge cycles. For Seville, this life is expected to be around 7-8 years.

An illustration of ACR’s performance is presented in Figure 2.

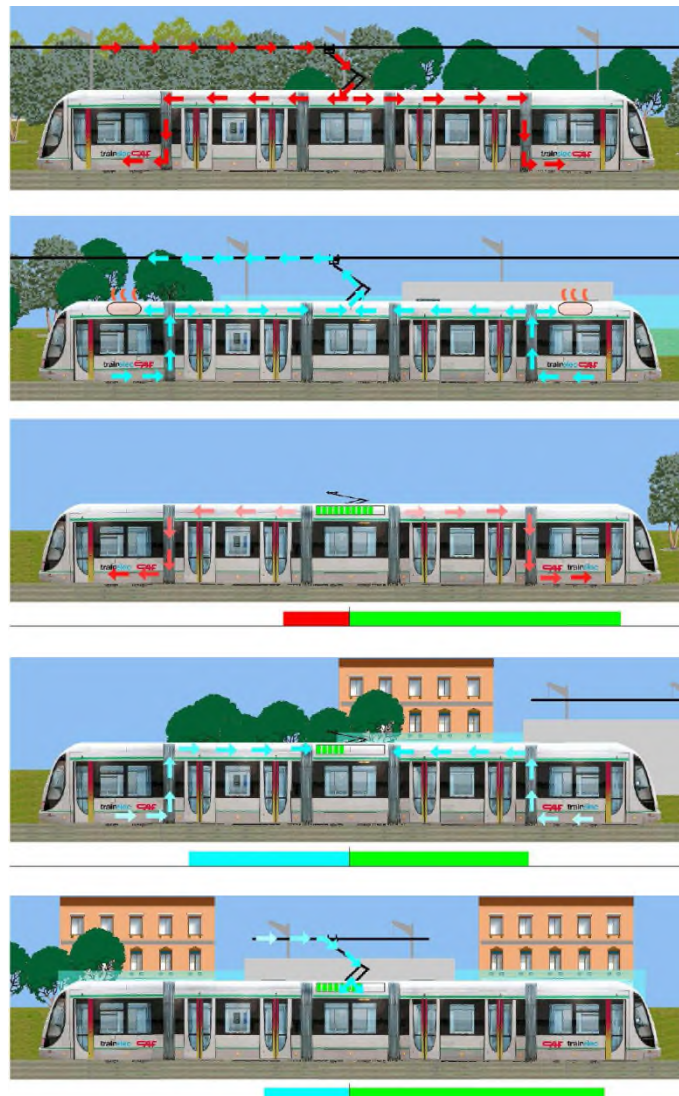


Figure 2: CAF’s APR technology. a) Tram without ACR running under overhead contact system. b) Trams without ACR braking. c) Tram with ACR running without overhead contact system. d) Tram with ACR braking and accumulating energy in ACR modules. e) Tram with ACR accumulating energy in a zone with overhead contact system

2. SIMULATION MODEL FOR THE ON-BOARD ENERGY STORAGE SYSTEM

With the on-board storage element on the CAF Urbos 3, the necessary electrical drive power can be provided by the storage element as shown in figure 3.

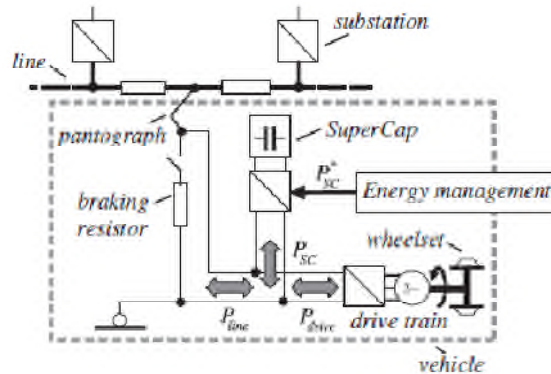


Figure 3: CAF Urbos 3 with ACR system

Many parameters influence the design of a supercapacitive **energy storage system** for the CAF Urbos 3. Features such as tram weight, passenger load, maximum speed, driving cycle, altitude differences and supercapacitor characteristics need to be studied to determine the **energy storage system** in terms of energy capacity. To evaluate the effects of all these parameters, a backwards looking simulation tool [4,5] has been developed in Matlab/Simulink with the objective of determining the power flow at tram level, line voltage and current, and power drawn from substations with and without on-board supercapacitors. Figure 4 shows a detail of the tram model inside the simulation program.

Starting from a predefined speed cycle, it calculates both the traction and braking power requested by the tram. Then, according to the requested power at the DC bus level, a power controller (blue), determines the amount of power to be provided by the supercapacitors and the remaining power to be provided from the net.

The power split will depend on parameters such as the total power requested, the state of charge of supercapacitors, the tram speed, overhead line voltage, etc. This can be done in many different ways depending on the strategy used and the objective to achieve. In our case, since the aim is to recover the braking energy, the power controller will make sure that for a certain speed, the state of charge of the supercapacitors will be appropriate to allocate the vehicle kinetic energy in case of sudden braking.

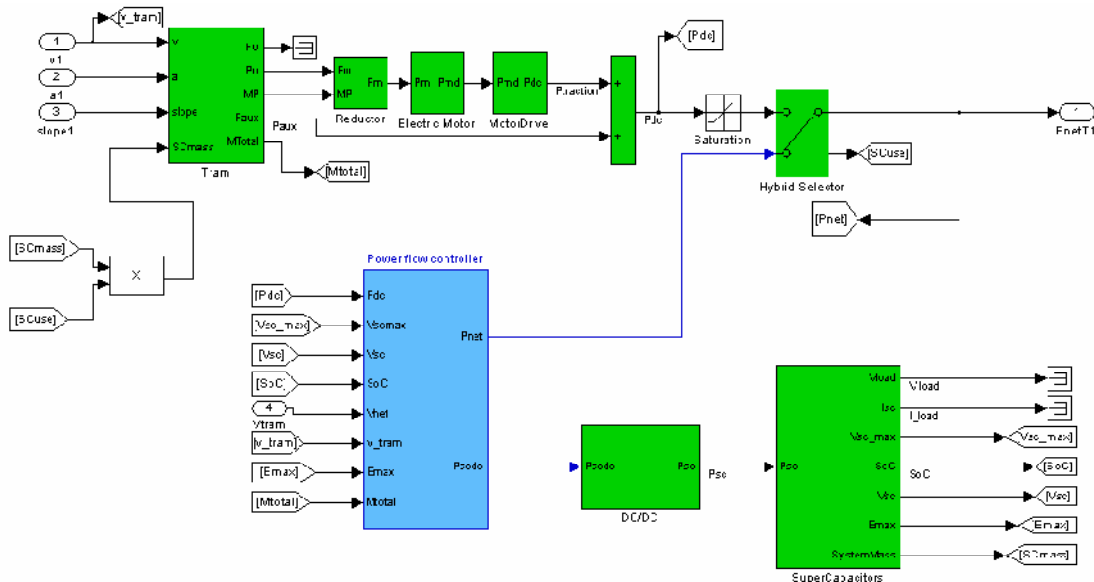


Figure 4: Detail of tram model in simulation program

The speed cycle considered for simulation tests is shown in Fig. 5 a) and lasts $T = 60s$ [x]. The simulated tram starts from standstill, accelerates up to $v_f = 65$ km/h (corresponding to a motor speed $\omega_m = 1250$ rpm), cruises for about eleven seconds and brakes for sixteen seconds until it stops. The whole cycle has been simulated for one stop for a total covered distance of 570 m (see figure 7 c). During the starting phase ($\Delta t \cong 24s$), the reference speed has been set to

$v_{t,ref} = 65$ km/h and the vehicle linearly accelerates (see figure 5 b) with a maximum traction effort set to $F_{t,max} = 340$ N (corresponding to a motor torque $T_{m,max} = 47$ Nm), as shown in figure 5 d).

2.1 Simulation results base without ACR system

In the exemplae that the lithium-ion capacitor energy storage system is not connected, the line current i_{sub} is equal to the tram current i_t , as shown in figure 5 a), and increase up to the peak value $i_{sub,peak}^{(BR)} = 17$ A and the tram voltage, V_t , drops from 535 V to 460 V, therefore having a maximum voltage drop of $\Delta V_{t,max}^{(BR)} = 75$ V that occurs at $t = 24$ s (see figure 6 b). In the same time instant, the substation output voltage V_{sub} is 494 V.

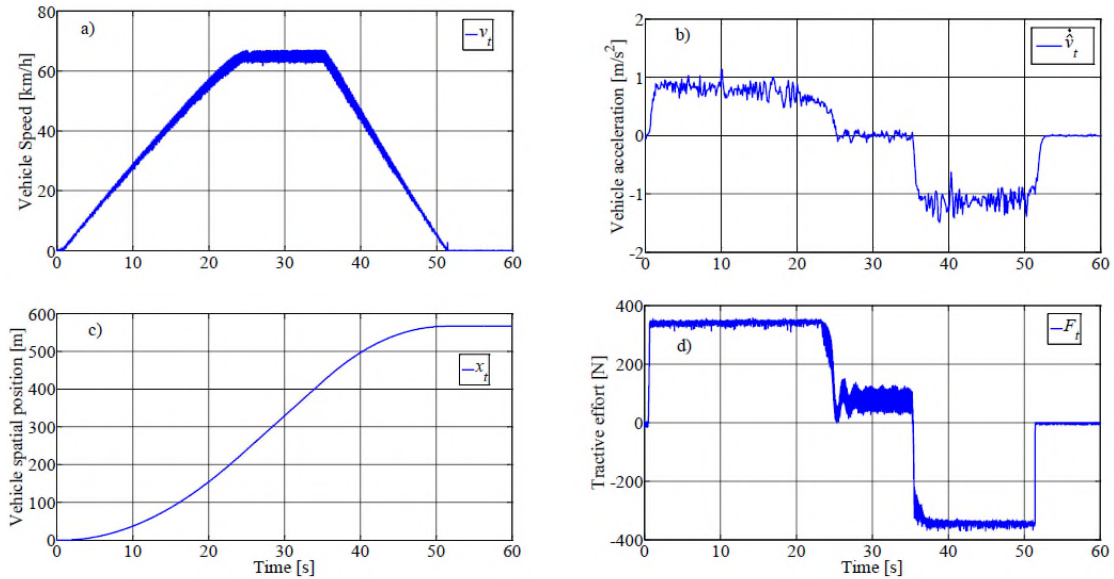


Figure 5: On-board base case simulation results: a) Tram speed; b) Tram estimated acceleration; c) Total distance covered by the tram; d) Tram traction effort

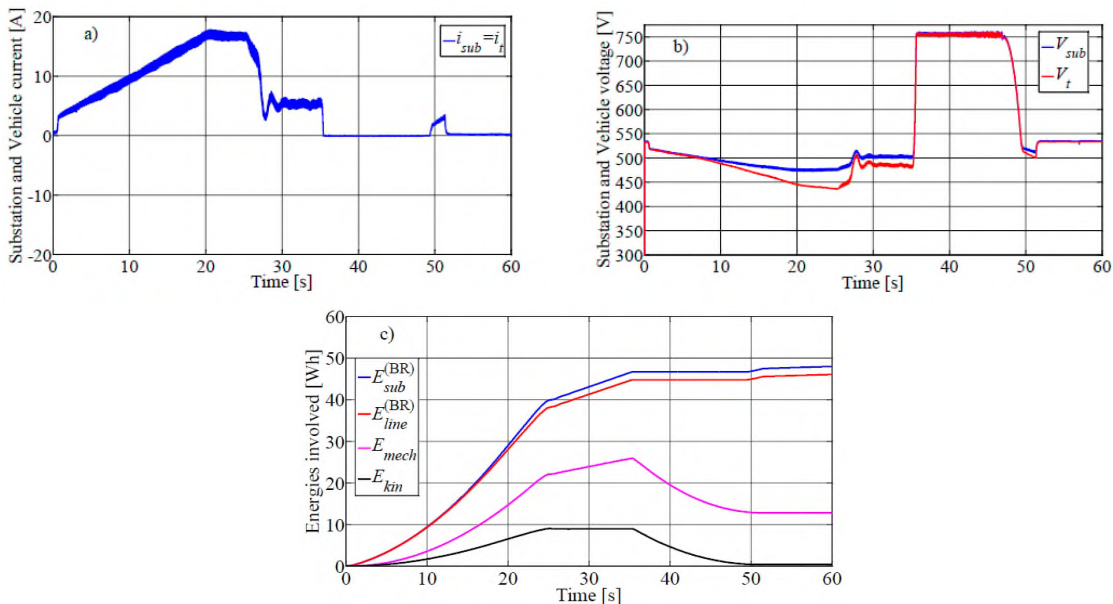


Figure 6: On-board base case simulation results: a) Line and tram currents; b) Substation and tram voltages; c) Energies involved with dissipative braking

Then the steady-state speed is reached, the tram current drops to $i_t = 5.4$ A and the tram voltage increases up to $V_t = 492$ V. Both the line and tram current present several oscillation due to mechanical torque vibrations. After the cruise, the speed reference is set to zero and the tram brakes with a constant effort equal to $F_b = -348$ N; the speed linearly

decreases until the tram stops. During the braking, the kinetic energy of the train is converted into electrical energy by the electrical traction drive. During the braking operation, since the AC/DC diode rectifier is unidirectional, the energy coming from the drive charges its DC-link capacitor, involving the increase of the vehicle voltage depicted in figure 6 b).

When the braking rheostat of the traction inverter is switched on, the tram voltage is limited to 750 V (dissipative braking).

The figure 6 c) depicts the energies involved during the traction cycle, where as the table reports their numerical values. In particular, $E_{sub}^{(BR)}$ denotes the energy supplied by the electrical substation, $E_{line}^{(BR)}$ evaluates the energy supplied by the catenary line, E_{mech} is the tram mechanical energy and E_{kin} is its kinetic energy. The total system losses E_{loss} are evaluated as the difference between the total input energy and the energy available at the tram’s wheel. These losses collect the overall electrical and mechanical losses, (i.e. energy lost on the line resistance, friction losses etc...). However, the eq. (1) shows how the aforementioned energies have been evaluated, in which the superscript “BR” refers to the energy values evaluated for this dissipative case base.

$$\begin{aligned}
 E_{sub}^{(BR)} &= \int_T V_{sub} \cdot i_{sub} \cdot dt \\
 E_{sub}^{(BR)} &= \int_T (V_{sub} \cdot i_{sub} - R_{line} \cdot i_{sub}^2) \cdot dt \\
 E_{mech} &= \int_T T_m \cdot \omega_m \cdot dt \\
 E_{kin} &= \int_T J_t \cdot \frac{d\omega_m}{dt} \cdot \omega_m \cdot dt \\
 E_{loss}^{(BR)} &= E_{sub}^{(BR)} - (E_{mech}) \operatorname{sgn}(T_m)
 \end{aligned} \tag{1}$$

The energy diagrams depicted in Fig. 6 c) are also summarized in Table 1.

Table 1: Cycle energy and losses evaluation in simulation results for case without ACR system

Energy [Wh]	Acceleration (at $t= 24.8$ s)	Cruise (at $t= 35.4$ s)	Braking (at $t= 51.5$ s)	Cycle
$E_{sub}^{(BR)}$	39,8	6,90	0,90	47,8
$E_{line}^{(BR)}$	38,1	6,68	0,82	45,6
E_{mech}	22,0	3,83	-13,0	12,8
E_{kin}	8,94	0,00	-8,94	0,00
E_{LiC}	-	-	-	-
$E_{loss}^{(BR)}$	17,8	3,07	14,1	35,0

In the case of no energy storage system on-board, at the end of acceleration, the total input energy is $E_{sub}^{(BR)} = 39.8Wh$, whose 1.7 Wh are lost on the contact line. The delivered mechanical energy is $E_{mech} = 22$ Wh, whose $E_{kin} = 8.94$ Wh are stored as kinetic energy of the vehicle. The total losses are computed in 17.8 Wh. During cruising, the kinetic energy is constant. The energy supplied by the substation is equal to 6.9 Wh and covers the mechanical and electrical energy losses, equal to 3.07 Wh. At the end of braking, the train stops and the input energy is equal to 13.9 Wh, whose 13.0 Wh is the mechanical energy available by the tram and 0.90 Wh is supplied by the line. The total energy losses in this phase is 14.1 Wh that has been partially dissipated on the braking rheostat $r_{BR,1}$.

At the end of the operating cycle, the total input energy is $E_{sub}^{(BR)} = 47.8Wh$ whereas the total losses results $E_{loss}^{(BR)} = 35,0Wh$. These values are taken as reference values for the further comparative analysis.

2.2 Simulation results base with ACR system

The ACR system are pre-charged to $V_{SC,max} = 135$ V. The behavior of the traction drive equipped with ACR system is evident from the compared analysis of figure 7 a) and figure 7 c). In particular, this last one shows that ACR reference current, $i_{SC,ref}$, change in sign according to vehicle acceleration. In fact, actual ACR current, $i_{SC,ref}$ reaches its maximum of 19.5 A at the maximum speed and falls to zero at the end of the acceleration. During the braking, a similar behavior

can be observed with the opposite current sign whose maximum results -33.6 A. The ACR current is reflected in the current supplied by the substation and that drawn by the dc-bus of the traction vehicle, i_t , shown in figure 7 a). The “peak shaving” action due to the contribution of ACR system is highlighted by the diagram of the substation current, i_{sub} , that in correspondence of $t= 24$ s, presents a peak equal to $i_{sub,peak}= 12.4$ A, significantly smoothed respect to one of the vehicle current, which is obviously the same as for the case of dissipative braking ($i_{sub,peak}^{(BR)} = 17$ A), with consequent current peak reduction by 27.1 %.

The figure 7 d) shows how ACR speed tracker control is capable of tracking quickly the ACR reference internal voltage, $u_{SC,ref}$, calculated according to the actual vehicle speed eq. (2).

$$u_{SC,ref} = f(\omega_{m,i}) = V_{SC,max} \sqrt{1 - \frac{\sum k_i \cdot J_{t,i} \cdot \omega_{m,i}^2}{C_{SC} \cdot V_{SC,max}^2}} \quad (2)$$

Where are: $J_{t,i}$ equivalent rotating inertia of motor axles of CAF Urbos 3, $V_{SC,max} = 136$ V, $k_i = 1$.

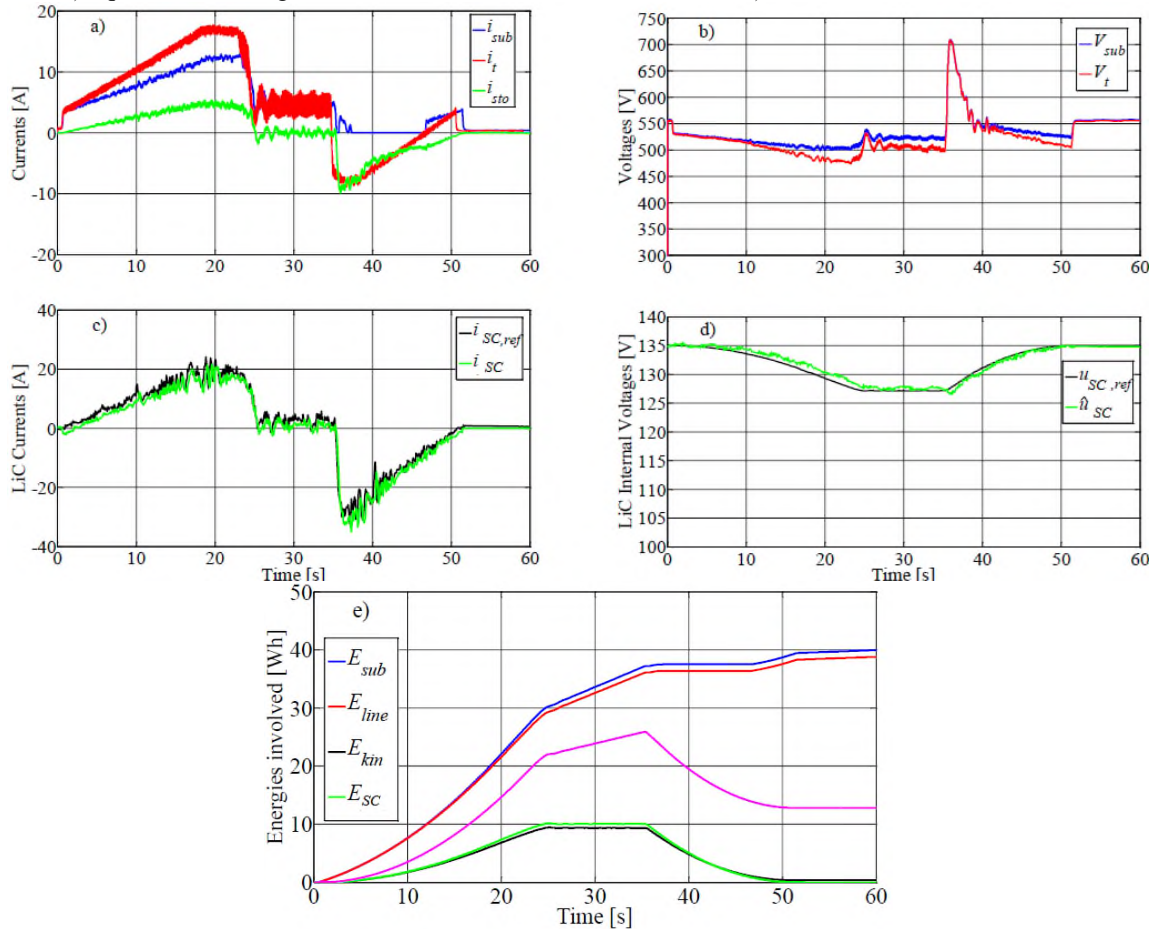


Figure 7: On-board with Rapid Charge Accumulator (ACR) system simulation results: a) Line, tram and storage currents; b) Substation and tram voltages; c) SC actual current and its reference; d) ACR internal estimated voltage and its reference; e) Energies involved in the traction cycle

In agreement with the suggested control strategy, ACR system reach the minimum voltage of 127 V when the simulated vehicle travels at the maximum speed.

During the braking, the kinetic energy is converted into electrical energy by the electrical traction drive, as it can be seen since i_t is negative. In this phase, ACR stores the electrical energy available and is recharged to its initial state of charge value since the ACR internal voltage reference is directly related to the actual vehicle kinetic energy E_{kin} , as it is evident from figure 7 e). This effect can be also highlighted in figure 7 d) by the increasing of ACR voltage when the braking starts.

As it is evident from the figure, the agreement between estimated (\hat{u}_{SC}) and reference ACR voltage is very good for all the cycle, confirming the effectiveness of the speed tracker control proposed.

The impact of the ACR system on the simulated railway DC electrified line is shown in Fig. 7 b). The voltage drop on the line, which occurs at $t=24$ s, is significantly reduced ($\Delta V_{t,\max} = 52V$) respect to the no-load substation voltage $V_{sub,0} = 535$ V) by the presence of ACR system for the whole duration of the acceleration.

The previous comments are supported by the diagram of the energies involved in the simulation test, reported in figure 9 e) and summarized in Table 2.

Table 2: Cycle energy and losses evaluation in simulation tests for the on-board with ACR system

Energy [Wh]	Acceleration (at $t=24.8$ s)	Cruise (at $t=35.4$ s)	Braking (at $t=51.5$ s)	Cycle
E_{sub}	30,3	7,20	2,40	39,9
E_{line}	29,3	6,80	2,20	38,3
E_{mech}	22,0	3,83	-13,0	12,8
E_{kin}	8,94	0,00	-8,94	0,00
E_{SC}	9,96	0,00	-9,96	0,00
E_{loss}	18,3	3,37	5,44	27,1

It has to be remarked that the energies evaluated by eq. (2) have to be redefined due to the presence of the on-board storage unit, which stores an energy denoted with E_{LIC} (3).

$$\begin{aligned}
 E_{sub} &= \int_T V_{sub} \cdot i_{sub} \cdot dt \\
 E_{line} &= \int_T (V_{sub} \cdot i_{sub} - R_{line} \cdot i_{sub}^2) \cdot dt \\
 E_{mech} &= \int_T T_m \cdot \omega_m \cdot dt \\
 E_{kin} &= \int_T J_t \cdot \frac{d\omega_m}{dt} \cdot \omega_m \cdot dt \\
 E_{SC} &= \int_T u_{SC} \cdot i_{SC} \cdot dt \\
 E_{loss} &= E_{sub} - (E_{mech})\text{sgn}(T_m) + (E_{SC})\text{sgn}(T_m)
 \end{aligned} \tag{3}$$

With reference to the acceleration phase, the total input energy is 40.26 Wh, whose 9.96 Wh have been supplied by ACR system and 30.3 Wh by the supply substation. and are equal to is 23.8 Wh. The total losses are computed in 18.3 Wh. During the cruise phase, the kinetic energy and the energy stored in ACR system are both constant and the energy supplied by the substation is equal to 7.2 Wh, which covers the line losses and the mechanical energy delivered to the vehicle, equal to 0.50 Wh and 3.83 Wh respectively.

At the end of the regenerative braking, the vehicle stops and the input energy is equal to 15.4 Wh, whose 13.0 Wh is the mechanical energy available by the vehicle and 2.40 Wh is supplied by the substation.

The energy actually stored in the ACR system is equal to 9.96 Wh which implies that they are re-charged up to their starting voltage. The total energy losses in this phase is 5.44 Wh. At the end of the operating cycle, the total input energy is $E_{sub}= 39.9$ Wh, whereas the total losses results $E_{loss}= 27.1$ Wh and it is evident that the comparison with the corresponding dissipative case (par. 3.1) shows that the total energy losses are decreased with consequent energy saving of about 16.5 %.

It is worth to be noted that the design of the simulator and the storage device has not been optimized for this specific traction cycle. Therefore, the energy saved can be further improved in a real system when the design of each device is oriented on the basis of the specific application.

3. COMPARISON FOR WITHOUT AND WITH THE ACR SYSTEM INSTALLATION

In order to better assess the differences and characteristics of the tested control strategies and also for remarking the benefit of installing the ACR system storage by evaluating the system performances in terms of energy efficiency improvement and voltage drops compensation, some specific performance indexes have been defined.

The table 3 shows the defined indexes by comparing all the aforementioned test results without and with the ACR system

Table 3: Performance indexes evaluation for on-board without and with the ACR system

Index	Without the ACR system	With the ACR system
Energy saving: $es\% = \left(1 - \frac{E_{sub}}{E_{sub}^{(BR)}}\right) \cdot 100$	-	16,5
Max Voltage drop: $\Delta V_{t,max}\% = \left(1 - \frac{V_{t,min}}{V_{sub,0}}\right) \cdot 100$	13,8**	9,91
Substation peak current reduction : $r_{sub,peak}\% = \left(1 - \frac{i_{sub,peak}}{i_{sub,peak}^{(BR)}}\right) \cdot 100$	-***	27,1

*Base value for the comparison $E_{sub}^{(BR)} = 47.8$ Wh,

** Base value for the comparison $\Delta V_{t,max}^{(BR)} = 75.0$ V with $V_{t,0} = V_{sub,0} = 535$ V,

*** Base value for the comparison $i_{sub,peak}^{(BR)} = 17.0$ A.

As it is clearly highlighted, on equal traction cycles, the ACR strategy assures the highest value of $es\%$ (**16.5 %**). This is mainly obtained thanks to the capability of the ACR technique to make null the energy wasted in the on-board braking rheostat. This is not a surprise, since the actual energy stored in the ACR system, E_{SC} , is instantly related to the actual kinetic energy of the vehicle, E_{kin} . The ACR strategy also gives satisfactory results with regard to maximum line voltage drop, $\Delta V_{t,max}\%$, and substation peak current reduction, $r_{sub,peak}\%$, which corresponds to the **9.91 %** of $V_{sub,0}$, (53 V) and the **27.1 %** of $i_{sub,peak}^{(BR)}$, (12.4 A).

The figure 10 shows the trend of the energy saving in function of the maximum cruise speed and different total distance covered, assuming the regenerative braking energy share coefficient: $\beta = 1$.

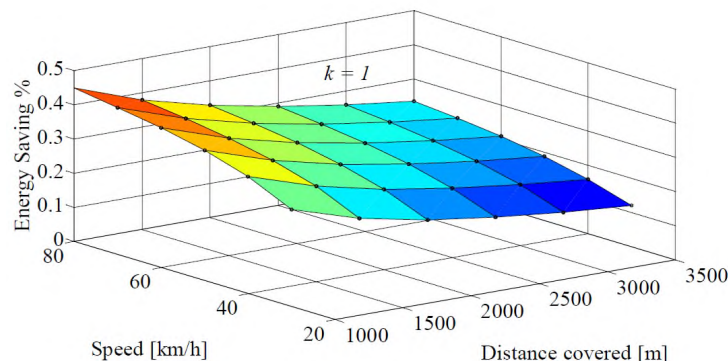


Figure 10: Trend of energy saving in function of the maximum vehicle speed and the total distance covered, with $\beta=1$

4. CONCLUSION

On board energy storage systems applied in the urban electrified public transport in Belgrade (R. Serbia) is still in a prototype state. Some open technical and commercial tasks have to be solved, but they seem to be uncritical. Nevertheless applications will not be done without any risk share between operator and vehicle manufacturer. Therefore it is too early to introduce energy storage in a bigger portion of new trams, but at least new vehicles should be prepared for the future. That means that vehicles for intensive usage - with a high energy saving potential - should be equipped with electrical traction equipment.

In spite of the mature technology of trams, many improvements concerning energy saving are still possible. The very different types of operation call for different methods of energy optimization. While the improvement of vehicle technology takes time and cost in general, the greatest effects will arise from a systematic and operational approach of the railway system based on sophisticated train control and management systems. As described in this research, the energy storage devices have reached a level of reliability that is necessary for transport application. Their benefits cover energy saving as well as improved system performance, together with possible reductions of greenhouse gas emission. In particular, intelligent control and management of auxiliary component can result in drastic reduction of energy

consumption during catenary-free operation of the trams. Local technical optimizations will result in smaller overall effects, most of which are attributable to the very mature level of technology that has been reached today.

REFERENCES

- [1] BARROW, K.: *Wireless connections*, International Railway Journal, Simmons Boardman Publishing Corporation, Cornwall, United Kingdom, June 2009.
- [2] THOMAS, G.: *The CAF Rapid Charge Accumulator: Technology for Removing Catenary Between Stations*, Tecrirail, Montané Comunicación S.L., Madrid, Spain, June 2009.
- [3] RODRÍGUEZ, A.: *Tranvía sin catenaria desarrollado por CAF y basado en el empleo de ultracondensadores*. Vía Libre, Fundación de los Ferrocarriles Españoles, Madrid, Spain, February 2009.
- [4] LÓPEZ-LÓPEZ T.J.; PECHARROMÁN R.R.; FERNÁNDEZ-CARDADOR A.; CUCALA A.P.: *Assessment of energy-saving techniques in direct-current-electrified mass transit systems*. Transportation Research Part C: Emerging Technologies, vol. 38, pp. 85-100, Jan. 2014.
- [5] GONZÁLEZ-GIL, A.; PALACIN, R., BATTY, P.: *Sustainable urban rail systems: Strategies and technologies for optimal management of regenerative braking energy*. Energy Conversion and Management, vol. 75, , pp. 374-388, 2013.
- [6] ADINOLFI, A., LAMEDICA, R.; MODESTO, C.; PRUDENZI, A.; VIMERCATI S.: *Experimental assessment of energy saving due to trains regenerative braking in an electrified subway line*. IEEE Trans. Power Delivery, vol. 13 (4), pp. 1536-1542, Oct. 1998.
- [7] RUFER A. : *Energy storage for railway systems, energy recovery and vehicle autonomy in Europe*. In: Proceedings of the international power electronics conference (IPEC'10), pp 3124–3127, Sapporo, Japan, 21–24 Jun 2010